CYK-4/GAP Provides a Localized Cue to Initiate Anteroposterior Polarity upon Fertilization

Noah Jenkins, *et al.*

Science **313**, 1298 (2006);
DOI: 10.1126/science.1130291

pump as well as for the transport of small molecules such as hexane (*27*, *28*). It is therefore proposed that besides the specific binding in the hydrophobic pocket of the T monomer, unspecific diffusion of small substrates through the observed tunnels occurs. Substrate transport from the membrane domain to the periplasmic tunnel might be via a lateral pathway, including the TM8/TM9 groove and the AcrA/AcrB interface. Recent reports (*25*, *26*) substantiate the close interaction between AcrA and AcrB (or of the homolog proteins MexA and MexB) in the tripartite complex, and we therefore anticipate conformational changes of AcrA coupled to those of AcrB. On the other hand, our structure does not support substrate transport through the central pore, as implied by the elevator mechanism (*14*, *17*), because access of substrates from the central cavity to the funnel is prohibited by the small diameter of the pore.

As AcrB is energized by the proton-motive force, transient protonation of titratable groups within the transmembrane domain of the protein can be expected to be the mechanism that delivers the energy required for the conformational changes described above. Indeed, we observe a prominent K940 (TM10) side-chain reorientation away from D408 and toward D407 (both on TM4) in the O conformation (Fig. 1B) and a bulging of TM5 toward TM4 and TM10, strengthening the hypothesis that this part of the transmembrane domain is central to proton binding and release (*16*, *19*). As thoroughly investigated in the case of bacteriorhodopsin (*5*–*7*, *29*), side-chain rearrangements (Fig. 1B) can leverage global conformational changes of the magnitude we observed for TM8 (fig. S3), involving reversible tilts of helices and the transient change of kinks and bulges in the main chain. We speculate that, in the case of AcrB, subtle changes in the transmembrane part (TM4 and TM10) produce the large conformational changes in the pore domain ultimately resulting in drug efflux. Different from what has been suggested for LacY (*30*) and EmrE (*31*), the proton and substrate translocation in AcrB appear to be spatially separated.

We have proposed a possible transport mechanism that, based on a functional rotation of the trimer, creates a peristaltic pump mechanism in each monomer (Fig. 3). Our model merges Jardetzky's alternate access pump (*32*) with the rotating site catalysis of F_1F_0-ATPase (*33*, *34*) and suggests a working hypothesis for the transport mechanism of RND transporters.

References and Notes

1. X. Z. Li, H. Nikaido, *Drugs* **64**, 159 (2004).
2. S. V. Ambudkar, I. W. Kim, Z. E. Sauna, *Eur. J. Pharm. Sci.* **27**, 392 (2006).
3. P. N. Markham, A. A. Neyfakh, *Curr. Opin. Microbiol.* **4**, 509 (2001).
4. K. Poole, *Clin. Microbiol. Infect.* **10**, 12 (2004).
5. J. K. Lanyi, *Mol. Membr. Biol.* **21**, 143 (2004).
6. H. Luecke, *Biochim. Biophys. Acta* **1460**, 133 (2000).
7. R. Neutze *et al.*, *Biochim. Biophys. Acta* **1565**, 144 (2002).
8. C. Toyoshima, G. Inesi, *Annu. Rev. Biochem.* **73**, 269 (2004).
9. J. Abramson *et al.*, *Science* **301**, 610 (2003).
10. Y. Huang, M. J. Lemieux, J. Song, M. Auer, D. N. Wang, *Science* **301**, 616 (2003).
11. D. Yernool, O. Boudker, Y. Jin, E. Gouaux, *Nature* **431**, 811 (2004).
12. D. J. Slotboom, I. Sobczak, W. N. Konings, J. S. Lolkema, *Proc. Natl. Acad. Sci. U.S.A.* **96**, 14282 (1999).
13. M. Grunewald, B. I. Kanner, *J. Biol. Chem.* **275**, 9684 (2000).
14. I. Sobczak, J. S. Lolkema, *Curr. Opin. Microbiol.* **8**, 161 (2005).
15. K. M. Pos, K. Diederichs, *Acta Crystallogr. Biol. Crystallogr.* **D58**, 1865 (2002).
16. S. Murakami, R. Nakashima, E. Yamashita, A. Yamaguchi, *Nature* **419**, 587 (2002).
17. E. W. Yu, G. McDermott, H. I. Zgurskaya, H. Nikaido, D. E. Koshland Jr., *Science* **300**, 976 (2003).
18. K. M. Pos, A. Schiefner, M. A. Seeger, K. Diederichs, *FEBS Lett.* **564**, 333 (2004).
19. L. Guan, T. Nakae, *J. Bacteriol.* **183**, 1734 (2001).
20. N. Tamura, S. Murakami, Y. Oyama, M. Ishiguro, A. Yamaguchi, *Biochemistry* **44**, 11115 (2005).
21. V. Koronakis, A. Sharff, E. Koronakis, B. Luisi, C. Hughes, *Nature* **405**, 914 (2000).
22. S. Murakami, N. Tamura, A. Saito, T. Hirata, A. Yamaguchi, *J. Biol. Chem.* **279**, 3743 (2004).
23. E. W. Yu, J. R. Aires, G. McDermott, H. Nikaido, *J. Bacteriol.* **187**, 6804 (2005).
24. J. Mikolosko, K. Bobyk, H. I. Zgurskaya, P. Ghosh, *Structure* **14**, 577 (2006).
25. D. Nehme, K. Poole, *Antimicrob. Agents Chemother.* **49**, 4375 (2005).
26. T. Touze *et al.*, *Mol. Microbiol.* **53**, 697 (2004).
27. D. G. White, J. D. Goldman, B. Demple, S. B. Levy, *J. Bacteriol.* **179**, 6122 (1997).
28. X. Z. Li, L. Zhang, K. Poole, *J. Bacteriol.* **180**, 2987 (1998).
29. B. W. Edmonds, H. Luecke, *Front. Biosci.* **9**, 1556 (2004).
30. O. Mirza, L. Guan, G. Verner, S. Iwata, H. R. Kaback, *EMBO J.* **25**, 1177 (2006).
31. N. Gutman, S. Steiner-Mordoch, S. Schuldiner, *J. Biol. Chem.* **278**, 16082 (2003).
32. O. Jardetzky, *Nature* **211**, 969 (1966).
33. J. P. Abrahams, A. G. Leslie, R. Lutter, J. E. Walker, *Nature* **370**, 621 (1994).
34. P. D. Boyer, *Annu. Rev. Biochem.* **66**, 717 (1997).

35. We thank the beamline staff at the Swiss Light Source (SLS) of the Paul Scherrer Institut in Villigen (Switzerland), and at the European Synchrotron Radiation Facility (ESRF) in Grenoble (France). This work was supported by a grant of the Transregio-Sonderforschungsbereich Zurich-Konstanz to K.D. We thank P. A. Karplus and W. Welte for critical reading and discussion. The atomic coordinates and structure factors of the C2 and P1 crystal forms have been deposited at the Protein Data Bank with accession numbers 2GIF and 2HRT, respectively. This work is dedicated to Peter Dimroth on the occasion of his 65th birthday.

Supporting Online Material

www.sciencemag.org/cgi/content/full/313/5791/1295/DC1
Materials and Methods
Figs. S1 to S3
Tables S1 and S2
References

20 June 2006; accepted 1 August 2006
10.1126/science.1131542

CYK-4/GAP Provides a Localized Cue to Initiate Anteroposterior Polarity upon Fertilization

Noah Jenkins,* Jennifer R. Saam,* Susan E. Mango‡

The *Caenorhabditis elegans* anteroposterior axis is established in response to fertilization by sperm. Here we present evidence that RhoA, the guanine nucleotide–exchange factor ECT-2, and the Rho guanosine triphosphatase–activating protein CYK-4 modulate myosin light-chain activity to create a gradient of actomyosin, which establishes the anterior domain. CYK-4 is enriched within sperm, and paternally donated CYK-4 is required for polarity. These data suggest that CYK-4 provides a molecular link between fertilization and polarity establishment in the one-cell embryo. Orthologs of CYK-4 are expressed in sperm of other species, which suggests that this cue may be evolutionarily conserved.

Many organisms depend on sperm entry to polarize the one-cell embryo. In *C. elegans*, sperm establish the anteroposterior axis and lead to asymmetric distribution of PAR-3 and PAR-6 to the anterior cortex (*1*). The prevailing view is that sperm modulate actomyosin contractility, which induces cortical flow toward the nascent anterior pole, thereby pulling PAR-3 and PAR-6 anteriorly (*2*–*4*). Two models could account for how contractile forces become asymmetric. One possibility is that sperm entry generates a physical disruption in the actomyosin network, enabling the network to pull away from the site of sperm entry. Alternatively, a component of sperm could control actomyosin contractility while leaving the network physically intact. Here we describe a sperm-donated factor that controls the actomyosin cytoskeleton and anterior PAR localization.

Our previous studies demonstrated that the guanosine triphosphatase (GTPase)–activating protein (GAP) *cyk-4* was critical to polarize epithelia (*5*, *6*). To investigate the role of *cyk-4*

Department of Oncological Sciences, Huntsman Cancer Institute, University of Utah, Salt Lake City, UT 84112, USA.

*These authors contributed equally to this work.
‡To whom correspondence should be addressed. E-mail: susan.mango@hci.utah.edu

during polarization, we examined the fertilized embryo, a well-characterized model for polarity (*2*). Antibody staining revealed that CYK-4 was dramatically enriched in sperm (64 out of 64 embryos examined) (Fig. 1, A and B). Inactivation of *cyk-4* by RNA interference (RNAi) indicated that staining was specific and RNAi effective (fig. S1) (*7*). Upon fertilization, CYK-4 could be detected at the posterior cortex of the one-cell embryo of both wild-type embryos and embryos lacking maternal CYK-4 (Fig. 1, C to K, and figs. S2 and S3) (*7*). We observed paternal CYK-4 in punctate structures, derived from sperm membranous organelles (MOs) and often associated with the sperm pronucleus (*8*). Based on nuclear morphology, paternal CYK-4 remained associated with the cortex and MOs during meiosis and the onset of polarity, a period of about 30 min (Fig. 1, C to K) (*2*).

To determine whether *cyk-4* was important for polarity, we examined anterior PAR proteins using green fluorescent protein (GFP) reporters in *cyk-4(RNAi)* embryos (Fig. 2, A and B) (*7*). In wild-type embryos, PAR-6::GFP was confined to 47% of egg length at the time of pronuclear meeting. In *cyk-4(RNAi)* embryos, PAR-6::GFP expanded to 87% of egg length, and endogenous PAR-3 was observed throughout the cortex (table S1 and fig. S4). These data suggest that *cyk-4* is required to establish anterior polarity.

In other organisms, *cyk-4* orthologs function with the guanine nucleotide exchange factor (GEF) *ect-2* during cytokinesis (*9*), which prompted us to examine *ect-2*. Antibody staining revealed that ECT-2 was enriched with nonmuscle myosin NMY-2::GFP at the cell cortex ($n > 20$) (Fig. 3). Colocalization of these two proteins in multiple images suggested that ECT-2 moves anteriorly coincident with NMY-2::GFP. Reduction of *ect-2* by RNAi indicated that staining was specific and RNAi effective (13 out of 16) (fig. S1). Inactivation of *ect-2* led to distribution of PAR-6::GFP and PAR-3 throughout the cortex at the time of pronuclear meeting, in addition to pronounced cytokinesis defects (Fig. 2C, and table S1 and fig. S4) (*7*). Because *ect-2* and *cyk-4* polarity phenotypes were visible before the first cell division, mislocalization of anterior PAR proteins was not a secondary consequence of failed mitosis. We conclude that *cyk-4* and *ect-2* are critical to establish the anterior PAR domain.

ect-2 and *cyk-4* are predicted to control Rho family GTPases, which suggested a possible mechanism for controlling polarity. In vitro, *cyk-4* can function as a GAP for *rhoA*, *cdc-42*, or *rac*, and in vivo, it likely controls RhoA during cytokinesis (*10*). We found that in embryos with reduced RhoA [*rho-1(RNAi)*], PAR-6::GFP was dispersed throughout the cortex at pronuclear meeting (Fig. 2D and table S1). This phenotype resembled that of *ect-2(RNAi)*, which suggested that ECT-2 and RHO-1 function in a common pathway. The similarity of phenotypes contrasts with those associated with other *C. elegans* GTPases. For example, *cdc-42* is required for posterior PAR localization and spindle positioning, but not for initial anterior PAR localization (*11*). No early polarity defects have been noted for the three *C. elegans rac* genes *ced-10*, *mig-2*, and *rac-2*, even when they were inactivated together (*12*). These observations suggest that RHO-1/RhoA is a good candidate effector for ECT-2 and, by extension, CYK-4 during the initial stages of polarization. We propose that the regulatory cassette of *rho-1*, *cyk-4*, and *ect-2* that is used during cytokinesis is also deployed for polarity.

Normally, anterior PAR localization depends on a gradient of actomyosin toward the anterior pole (*3*, *4*). Because Rho proteins control the actomyosin cytoskeleton in many contexts, we examined the actomyosin cytoskeleton with nonmuscle myosin NMY-2::GFP. In wild-type embryos, NMY-2::GFP was present at the egg cortex, where it formed coalescing foci that advanced anteriorly (Fig. 4, A to C) (*7*). In 7 out of 10 *ect-2(RNAi)* and 6 out of 8 *rho-1(RNAi)* embryos, a lower proportion of NMY-2::GFP localized cortically, and this remaining protein failed to coalesce into large foci (Fig. 4, D to I) (*7*). These data suggest that *ect-2* and *rho-1* are critical to generate a contractile actomyosin network.

Conversely, *cyk-4* controlled relaxation or disassembly of the actomyosin network. Of 30 *cyk-4(RNAi)* embryos, 15 had a dynamic actomyosin network that remained evenly distributed over the cortex (Fig. 4, J to L) (*7*). In these embryos, initial contractility appeared wild type but sperm-induced asymmetry was lost. In 10 out of 30, asymmetric NMY-2::GFP occurred, but the global transition from foci to puncta was delayed until after pronuclear meeting, which suggested a temporal role for *cyk-4* (fig. S5) (*7*). The remaining 5 out of 30 embryos had an intermediate phenotype (fig. S6) (*7*). The variable *cyk-4(RNAi)* phenotypes could reflect incomplete inactivation by RNAi or the existence of additional polarity pathways.

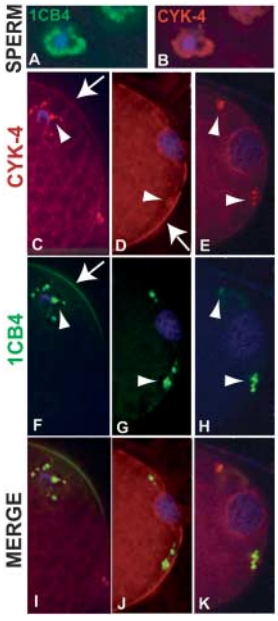

Fig. 1. CYK-4 is enriched in sperm. (**A** and **B**) Endogenous CYK-4 (red) localizes within sperm, which are costained with the membranous organelle marker 1CB4 (green) (*8*, *25*); DNA is blue. Paternal CYK-4 in embryos (**C** to **K**): embryos that are maternally *cyk-4(RNAi)* but paternally CYK-4+. [(C), (F), and (I)] before meiosis; [(D), (G), and (J)] undergoing meiosis II; [(E), (H), and (K)] post meiosis, with polarity initiation. Paternal CYK-4 is at the posterior cortex (arrows) and in membranous organelles (arrowheads). Anterior is left and embryos are ~50 μm long.

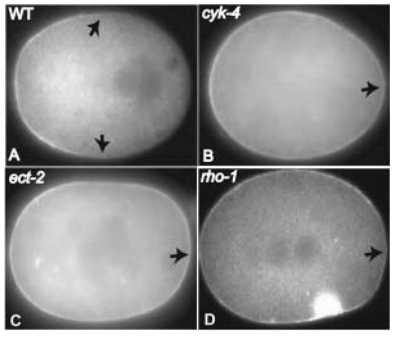

Fig. 2. Anterior localization of PAR-6::GFP depends on *cyk-4*/GAP, *ect-2*/GEF, and *rho-1*/RhoA. Compared with the wild type (WT) (**A**), PAR-6::GFP is expanded in *cyk-4(RNAi)* (**B**), *ect-2(RNAi)* (**C**), and *rho-1(RNAi)* (**D**) embryos. Arrows denote end points of PAR-6::GFP.

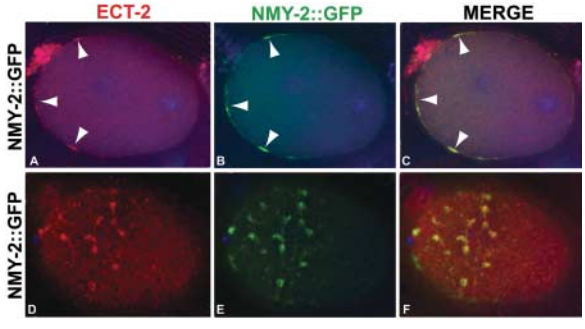

Fig. 3. ECT-2 localizes to the cortex and is coincident with NMY-2::GFP. (**A** and **D**) Endogenous ECT-2 (red) is enriched in puncta at the cell cortex. (**B** and **E**) These puncta colocalize with NMY-2::GFP (green); (**C** and **F**) merge is yellow. (A) to (C) are cross sections; (D) to (F) are surface shots. On the basis of nuclear morphology and position, embryos are undergoing pronuclear migration.

Supporting the former hypothesis, we detected CYK-4 protein in 39% of sperm after RNAi treatment (fig. S6) (*7*). These data suggest that *cyk-4* is required to down-regulate the actomyosin cytoskeleton posteriorly and, thereby, to induce asymmetric pulling forces.

One effector of RhoA is RhoA kinase, which phosphorylates myosin light chain (MLC) and MLC phosphatase, which leads to MLC activation and actomyosin contractility (*13*). In *C. elegans*, MLC-4 is required for anteroposterior polarity, actomyosin contractility, and anterior PAR localization (*14*). These observations suggested that RHO-1, ECT-2, and CYK-4 might control MLC-4. To test this idea, we monitored activated MLC using an antibody specific for phospho-MLC (*7*, *13*).

Phospho-MLC was located at the cell cortex of wild-type embryos, where it overlapped with foci of NMY-2::GFP (Fig. 5, A and B, and fig. S7) (*7*). We detected phospho-MLC associated with the anterior cortex and absent from the posterior after fertilization, indicating loss of active MLC (fig. S8) (*7*). Loss of immunoreactivity in *mlc-4*(–) embryos indicated that phospho-MLC staining was specific (fig. S9) (*7*). Phosphorylation of MLC required *ect-2* and *rho-1*, since neither *ect-2(RNAi)* ($n > 10$) nor *rho-1(RNAi)* ($n = 7$ out of 9) embryos had detectable phospho-MLC at the cell cortex (Fig. 5, C and G, and fig. S7) (*7*). As predicted, *cyk-4(RNAi)* embryos contained phospho-MLC, which colocalized with NMY-2::GFP in an extended domain ($n > 10$ one-cell embryos with meiotic defects) (Fig. 5E and fig. S8) (*7*). These findings suggest that ECT-2 and RHO-1 promote, whereas CYK-4 inhibits, activated MLC and, therefore, actomyosin contractility.

To address the importance of sperm-donated CYK-4, we examined embryos from *NMY-2::GFP* females mated with *cyk-4(RNAi)* males (*7*). As monitored by NMY-2::GFP, 29% lacked polarity altogether, whereas 17% had an intermediate phenotype ($n = 48$) (Fig. 6, D and E); the remainder looked wild type. By antibody staining, 42% of sperm had reduced or absent CYK-4 after RNAi ($n = 90$) (Fig. 6B). These data indicate that paternally endowed CYK-4 is required to polarize the embryo. Conversely, we showed CYK-4+ from male sperm could rescue polarity, but not meiotic cytokinesis, for fertilized *cyk-4(RNAi)* eggs (figs. S10 and S11).

We propose that the bolus of CYK-4 donated by sperm down-regulates the actomyosin network in the posterior, thereby generating a gradient of contractility (fig. S12) (*7*). The gradient of contractility depends on differential activation of MLC. There may be additional effectors, given that RhoA in other organisms influences the actin cytoskeleton in multiple ways. In addition to CYK-4, previous studies have shown that the sperm-donated centrosome is required for anteroposterior polarity (*1*, *15*, *16*). Currently, it is unclear whether CYK-4 acts in parallel to the centrosome or whether these two sperm cues function in a common pathway. We note that the requirement for a mature centrosome helps explain why polarity initiates after the completion of meiosis, despite the presence of paternal CYK-4 immediately after fertilization.

Consistent with the model that RhoA, CYK-4, and ECT-2 function during the earliest stage of polarization, we observed the strongest polarity defects during the first half of the first cell cycle (table S1) (*7*). Subsequently, anterior PAR proteins and CDC-42 contribute to actomyosin dynamics (*3*, *4*, *17*). PAR-2 may function even later or in parallel, because anterior PAR are localized normally in *par-2* mutant embryos (*18*). Thus, polarization during the first cell cycle involves multiple stages governed by distinct sets of factors.

Our studies may also have implications for the role of CYK-4 during cytokinesis. Although the spindle midzone is a target of CYK-4 (*9*), recent studies revealed that a visible spindle midzone is not essential for cytokinesis (*19*, *20*). We suggest that the cortical actomyosin cytoskeleton may be a focus of CYK-4 during cytokinesis as it is during polarization.

Organisms such as tunicates and teleosts undergo asymmetric actomyosin contraction upon fertilization, which contributes to polarization of the fertilized egg (*21*). In *P. mammillata*, contraction depends on an actomyosin basket with its opening located at the site of sperm entry. Thus, asymmetry in these embryos may

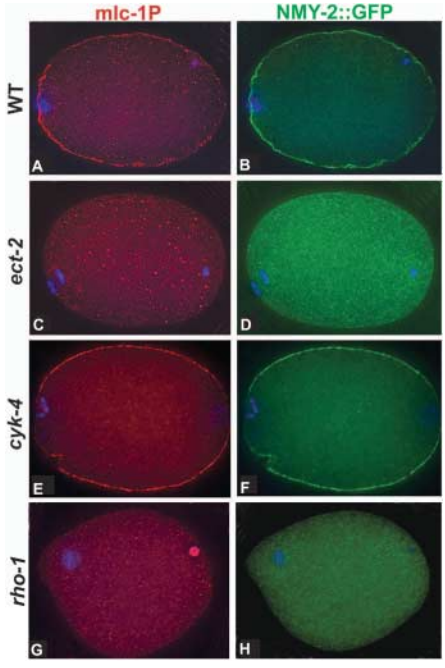

Fig. 5. Phospho-MLC localized at the cortex during polarization. (**A** and **B**) In wild-type (WT) embryos, antibodies that recognize phospho-MLC (mlc-1P, red) detect activated, endogenous MLC at the cell cortex, colocalized with NMY-2::GFP (green). In *ect-2(RNAi)* (**C** and **D**) and *rho-1(RNAi)* (**G** and **H**) embryos, phospho-MLC is rarely detected. (**E** and **F**) *cyk-4(RNAi)* embryos exhibit phospho-MLC throughout the cortex, with NMY-2::GFP. DNA is blue.

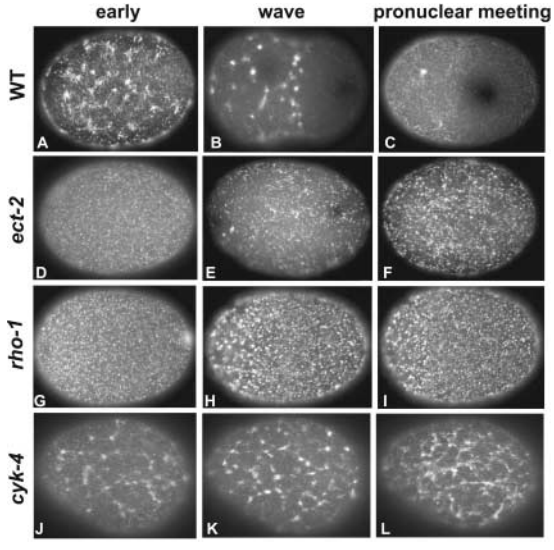

Fig. 4. *ect-2/GEF*, *rho-1/rhoA*, and *cyk-4/GAP* regulate the actomyosin wave. In wild-type (WT) embryos, a meshwork of nonmuscle myosin NMY-2::GFP (**A**, early) is enriched anteriorly during pronuclear migration (**B**, wave) and subsequently disperses into puncta at pronuclear meeting (**C**). In *ect-2(RNAi)* embryos (**D** to **F**) and *rho-1(RNAi)* embryos (**G** to **I**), contractile foci are rarely observed at any stage. In *cyk-4(RNAi)* embryos, 50% of embryos remain contractile over the entire embryo at all stages (**J** to **L**).

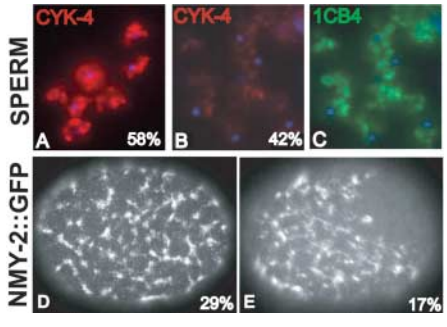

Fig. 6. Paternal *cyk-4* is required for polarity. Sperm from *cyk-4(RNAi); him-8* males exhibit reduced CYK-4 (**B**), while others appear unaffected (**A**). Sperm were counterstained for membranous organelles (1CB4) (**C**). Embryos from *NMY-2::GFP; fem-1* females and *cyk-4(RNAi); him-8* males exhibit loss of polarized NMY-2::GFP (**D**), or have a partial defect (**E**).

depend on the geometry of the actomyosin network rather than modulation of RhoA (*21*). On the other hand, animals with an even distribution of cortical actin may use orthologs of *rho-1*, *ect-2*, and *cyk-4* to modulate actomyosin configuration, analogous to *C. elegans*. Intriguingly, the *cyk-4* ortholog MgcRacGAP, is named for its enrichment in male germ cells in humans and *Drosophila* (*22*, *23*). In *Drosophila*, sperm entry is dictated by the position of the egg's micropyle, and therefore, a possible role for sperm in axis formation has not been addressed. One possibility is that *Drosophila* sperm contribute to embryonic polarity, and the stereotyped entry-point enables the egg and sperm to coordinate their polarizing activities. In mammals, there is debate regarding when polarity is established and the potential role of sperm (*24*). An exciting avenue for future investigation will be to determine whether other animals use CYK-4, RhoA, and ECT-2 to establish embryonic polarity in response to sperm.

References and Notes

1. B. Goldstein, S. N. Hird, *Development* **122**, 1467 (1996).
2. S. Q. Schneider, B. Bowerman, *Annu. Rev. Genet.* **37**, 221 (2003).
3. E. Munro, J. Nance, J. R. Priess, *Dev. Cell* **7**, 413 (2004).
4. R. J. Cheeks *et al.*, *Curr. Biol.* **14**, 851 (2004).
5. M. F. Portereiko, J. Saam, S. E. Mango, *Curr. Biol.* **14**, 932 (2004).
6. M. F. Portereiko, S. E. Mango, *Dev. Biol.* **233**, 482 (2001).
7. Materials and methods and additional data are available as supporting material on *Science* Online.
8. H. Okamoto, J. N. Thomson, *J. Neurosci.* **5**, 643 (1985).
9. M. Glotzer, *Science* **307**, 1735 (2005).
10. V. Jantsch-Plunger *et al.*, *J. Cell Biol.* **149**, 1391 (2000).
11. C. R. Cowan, A. A. Hyman, *Annu. Rev. Cell Dev. Biol.* **20**, 427 (2004).
12. E. A. Lundquist, P. W. Reddien, E. Hartwieg, H. R. Horvitz, C. I. Bargmann, *Development* **128**, 4475 (2001).
13. K. Riento, A. J. Ridley, *Nat. Rev. Mol. Cell Biol.* **4**, 446 (2003).
14. C. A. Shelton, J. C. Carter, G. C. Ellis, B. Bowerman, *J. Cell Biol.* **146**, 439 (1999).
15. P. L. Sadler, D. C. Shakes, *Development* **127**, 355 (2000).
16. C. R. Cowan, A. A. Hyman, *Nature* **431**, 92 (2004).
17. M. Gotta, M. C. Abraham, J. Ahringer, *Curr. Biol.* **11**, 482 (2001).
18. A. A. Cuenca, A. Schetter, D. Aceto, K. Kemphues, G. Seydoux, *Development* **130**, 1255 (2003).
19. K. J. Verbrugghe, J. G. White, *Curr. Biol.* **14**, 1755 (2004).
20. S. E. Encalada, J. Willis, R. Lyczak, B. Bowerman, *Mol. Biol. Cell* **16**, 1056 (2005).
21. F. Prodon, G. Pruliere, J. Chenevert, C. Sardet, *Med. Sci. (Paris)* **20**, 526 (2004).
22. A. Toure *et al.*, *J. Biol. Chem.* **276**, 20309 (2001).
23. M. Agnel, L. Roder, C. Vola, R. Griffin-Shea, *Mol. Cell. Biol.* **12**, 5111 (1992).
24. M. Zernicka-Goetz, *Nat. Rev. Mol. Cell Biol.* **6**, 919 (2005).
25. S. W. L'Hernault, in *C. elegans II*, D. L. Riddle, T. Blumenthal, B. J. Meyer, J. R. Priess, Eds. (Cold Spring Harbor Laboratory Press, Plainview, NY, 1997), vol. 1, pp. 271–294.

26. We thank M. Babst, M. Glotzer, J. Nance, J. Priess, B. Bowerman for reagents; and A. Schier, J. Rosenblatt, and laboratory members for reading the manuscript. Some strains were supplied by the *Caenorhabditis* Genetics Center, imaging was performed at the University of Utah Cell Imaging Facility. Oligo synthesis and DNA sequencing were supported by CCSG 2P30CA42014. This work was funded by K01DK02966-2 to J.R.S. S.E.M. was supported by NIH R01 GM056264, the Huntsman Cancer Institute, and Department of Oncological Sciences.

Supporting Online Material

www.sciencemag.org/cgi/content/full/1130291/DC1
SOM Text
Table S1
Figs. S1 to S12
Movies S1 to S5
References

22 May 2006; accepted 19 July 2006
Published online 27 July 2006;
10.1126/science.1130291
Include this information when citing this paper.

The Mevalonate Pathway Controls Heart Formation in *Drosophila* by Isoprenylation of Gγ1

Peng Yi,* Zhe Han,*† Xiumin Li, Eric N. Olson†

The early morphogenetic mechanisms involved in heart formation are evolutionarily conserved. A screen for genes that control *Drosophila* heart development revealed a cardiac defect in which pericardial and cardial cells dissociate, which causes loss of cardiac function and embryonic lethality. This phenotype resulted from mutations in the genes encoding HMG-CoA reductase, downstream enzymes in the mevalonate pathway, and G protein Gγ1, which is geranylgeranylated, thus representing an end point of isoprenoid biosynthesis. Our findings reveal a cardial cell–autonomous requirement of Gγ1 geranylgeranylation for heart formation and suggest the involvement of the mevalonate pathway in congenital heart disease.

Mutations in genes controlling heart development frequently cause fatal cardiac malformations, the most common type of birth defect in humans. Because many of the mechanisms involved in heart development are evolutionarily conserved, the fruit fly *Drosophila melanogaster* represents a powerful model for genetically dissecting this complex developmental process. The *Drosophila* heart, or dorsal vessel, which pumps bloodlike cells through an open circulatory system, is composed of parallel rows of contractile cardial cells (cardioblasts) tightly attached to pericardial cells; the latter perform supportive and secretory functions (Fig. 1A) (*1*).

We performed a P-element genetic screen (*2*) for *Drosophila* mutants with heart defects using transgenic flies harboring a green fluorescent protein (GFP) transgene under control of the *Hand* enhancer (*3*), which is specific for cardial cells, pericardial cells, and the lymph gland—a hematopoietic organ in fruit flies (Fig. 1B). The *Hand*-GFP transgene allows visualization of the developing heart at single-cell resolution. Among a collection of mutants with cardiac abnormalities, we observed a heart defect in which pericardial cells dissociated from cardioblasts in the dorsal vessel at the end of embryogenesis. We termed this phenotype "broken hearted" (bro). Here, we describe five such mutants of different genetic loci (Fig. 1, C to G). In contrast to the wild-type dorsal vessel in which the pericardial cells are intimately associated with cardioblasts, in each of these mutants, the relative positions of pericardial cells and cardioblasts changed with each heartbeat.

The P element in the *bro1* locus [l(3)01152] is located in the first exon of the *hydroxymethyl-*

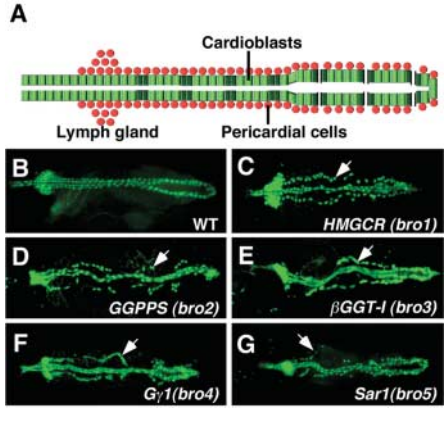

Fig. 1. Mutants in different genetic loci gave rise to a common broken hearted (bro) cardiac defect. (**A**) Schematic drawing of a late stage 17 embryonic heart (dorsal view, anterior to the left). (**B** to **G**) Stage 17 embryonic heart labeled by Hand-GFP (*3*) in wild-type embryo (B) or five bro homozygous mutants [(C) to (G)] (pericardial cells are indicated by arrows) (C) *HMGCR*, *bro1*, [l(3)01152]; (D) *GGPPS/qm*$^{L14.4}$, *bro2*; (E) β*GGT-I*$^{S-2554}$, *bro3*; (F) *Gγ1*, *bro4*, [l(2)k08017]. (G) *Sar1*, *bro5*, [l(2)k07408].

Department of Molecular Biology, University of Texas Southwestern Medical Center, 6000 Harry Hines Boulevard, Dallas, TX 75390–9148, USA.

*These authors contributed equally to this work.
†To whom correspondence should be addressed. E-mail: zhe.han@utsouthwestern.edu (Z.H.); eric.olson@utsouthwestern.edu (E.N.O.)